

# Charge transfer and formation of conducting C<sub>60</sub> monolayers at C<sub>60</sub>/noble-metal interfaces

Ryo Nouchi<sup>a)</sup> and Ikuo Kanno

Department of Nuclear Engineering, Graduate School of Engineering, Kyoto University, Yoshidahonmachi, Sakyo, Kyoto 606-8501, Japan

(Received 22 November 2004; accepted 28 February 2005; published online 5 May 2005)

The resistance of a conducting C<sub>60</sub> monolayer formed on a polycrystalline Ag film was found to be  $0.7 \pm 0.1$  k $\Omega$  by *in situ* resistance measurements. By another series of *in situ* resistance measurements, the surface scattering cross sections, whose magnitude represents the relative amount of transferred charge, were evaluated as 100 Å<sup>2</sup> for C<sub>60</sub>/Au, and 150 Å<sup>2</sup> for C<sub>60</sub>/Cu and C<sub>60</sub>/Ag systems. However, comparison with previous results obtained for monolayers formed on Au and Cu films showed that the resistances of conducting C<sub>60</sub> monolayers do not show a simple dependence on the transferred charge. Atomic force microscopy measurements revealed that the grain size of the underlying noble metals also plays an important role. © 2005 American Institute of Physics. [DOI: 10.1063/1.1897840]

## I. INTRODUCTION

Charge transfer from metal atoms to C<sub>60</sub> molecules plays a major role in determining physical and chemical properties of C<sub>60</sub>-metal systems. This charge transfer is caused by the high electron affinity of C<sub>60</sub>, where C<sub>60</sub> molecules act as electron acceptors. In alkali fullerenes, there is complete charge transfer from the metal atoms to the lowest unoccupied molecular orbital (LUMO) of C<sub>60</sub> molecules. On the other hand, in C<sub>60</sub>-noble-metal systems, only fractional filling of the LUMO occurs because noble metals have higher work functions than alkali metals. These charge-transfer effects give rise to conductivity in C<sub>60</sub> molecules.

When C<sub>60</sub> is deposited onto thin noble-metal films, a bilayer structure is formed: noble metals have higher cohesive energies than alkali metals, and cannot be intercalated into the C<sub>60</sub> lattice as is the case with alkali fullerenes. Electrons transfer to the adjacent C<sub>60</sub> monolayer<sup>1-3</sup> from the noble-metal atoms and form a conducting C<sub>60</sub> monolayer. In a previous work, the authors performed *in situ* resistance measurements of C<sub>60</sub>/Au and C<sub>60</sub>/Cu bilayer structures and reported that the resistances of conducting C<sub>60</sub> monolayers formed on polycrystalline Au and Cu films were  $0.9 \pm 0.2$  and  $2.4 \pm 0.4$  k $\Omega$ , respectively.<sup>4</sup> The *in situ* resistance measurements<sup>4-11</sup> enabled us to observe the charge transfer by inspecting the change in sheet resistance while depositing C<sub>60</sub> on thin metal films or vice versa.

The charge state of a C<sub>60</sub> molecule determines the electrical properties of the molecule. The difference in the resistances of conducting C<sub>60</sub> monolayers formed on Au and Cu films would reflect the difference in the number of electrons transferred from the underlayer metals to the LUMO of C<sub>60</sub> molecules. Hebard *et al.*<sup>10</sup> estimated the surface scattering cross section of C<sub>60</sub> adsorbates on a Cu film by means of *in situ* resistance measurements. The magnitude of the cross section represents the relative amount of transferred charge because conduction electrons in the metal underlayer feel

the charge transfer as an increase in the surface scattering potential.

In this article, we report on the results of three stages of experiments. First, the resistance of a conducting C<sub>60</sub> monolayer on a polycrystalline Ag film was determined by means of *in situ* resistance measurements. In order to discuss the results in comparison with the previously obtained ones for conducting C<sub>60</sub> monolayers on Au and Cu, the amount of transferred charge and the surface morphology of the metal layer, which determine the resistance of the conducting monolayer, should be known. In the second stage, another series of *in situ* resistance measurements to investigate the relationship between the work function of the underlying metal and the scattering cross section was carried out. This series of measurements tells us whether the charge transfer is simply dependent on the work function of the underlayer or not. Third, atomic force microscopy (AFM) measurements of noble-metal underlayers were carried out. By AFM measurements, we can observe the surface morphology of the metal underlayer.

## II. EXPERIMENT

We performed *in situ* resistance measurements while depositing C<sub>60</sub> molecules on polycrystalline noble-metal (Au, Cu, and Ag) films. In addition, in order to observe the surface morphology of the metal underlayer, AFM measurements were carried out for these three noble-metal films. Experimental details for these measurements are as follows.

All deposition and resistance measurements were performed at room temperature in a vacuum chamber which could be pumped to a base pressure of  $8 \times 10^{-7}$  Torr. This vacuum chamber had two heat sources for the evaporation of noble metals and C<sub>60</sub> molecules, a shutter and a quartz oscillation device. To eliminate any possible residual solvent in C<sub>60</sub> powder, the powder was heated for several hours at a temperature of about 200 °C in the vacuum chamber (below  $10^{-5}$  Torr) before deposition. A quartz glass with dimensions of 1 cm × 1 cm was used as the substrate. On the quartz

<sup>a)</sup>Electronic mail: nouchi@nucleng.kyoto-u.ac.jp

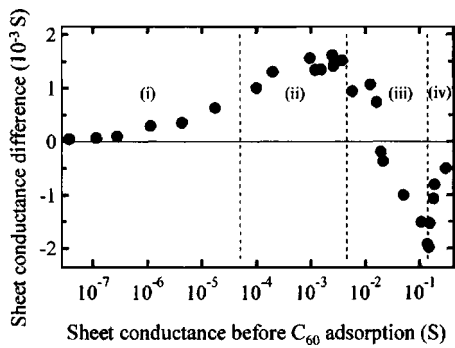


FIG. 1. Change in the sheet conductance of a  $C_{60}$ /Au bilayer film. The vertical axis represents the differences in sheet conductances before and after  $C_{60}$  deposition. The change has four stages with respect to the conductances of Au underlayers, i.e., with respect to the degree of underlayer metal growth.

substrate, four parallel electrodes made of Au (1 mm  $\times$  8 mm  $\times$  30 nm) were fabricated with 1-mm distances between them, for the four-probe method. A thin noble-metal film was deposited onto the electrodes by thermal heating of a W boat. After this process,  $C_{60}$  was deposited onto the noble-metal underlayer by thermal heating of a Mo boat. During  $C_{60}$  deposition, *in situ* resistance measurements were performed by the four-probe method. We monitored the average film thickness and the deposition rate using the quartz oscillation device. Details of the resistance measurements have been described previously.<sup>4</sup>

All AFM measurements of noble-metal underlayers were conducted on an SPI3800N/SPA400 probe station (Seiko Instruments Inc.) in contact mode. These measurements were performed in air at room temperature. All samples were 50-nm-thick films on quartz glass substrates and were fabricated in the vacuum chamber described above. These films were deposited by thermal heating of a W boat with the same deposition rate. All depositions were done at room temperature.

### III. RESULTS AND DISCUSSION

#### A. General features of changes in sheet conductance resulting from $C_{60}$ deposition

The deposition of  $C_{60}$  molecules on a thin noble-metal film dramatically changes the sheet resistance/conductance compared to when noble-metal atoms are deposited successively. Figure 1 shows the change in the sheet conductance of a  $C_{60}$ /Au bilayer film, as a function of the conductances of the Au underlayers. The values on the vertical axis represent the differences in sheet conductances before and after  $C_{60}$  deposition. The conductance of the Au underlayer is an index of the degree of the Au film growth. The change in sheet conductance has four stages with respect to the degree of underlayer metal growth.

In stage (i), enhancement of the conduction between metal islands is dominant. Such island formation is seen in the early stage of noble-metal film growth on insulating substrates. This effect is dominant for ultrathin noncontinuous films whose conduction is thermally active, and it increases the sheet conductance (decreases the sheet resistance). How-

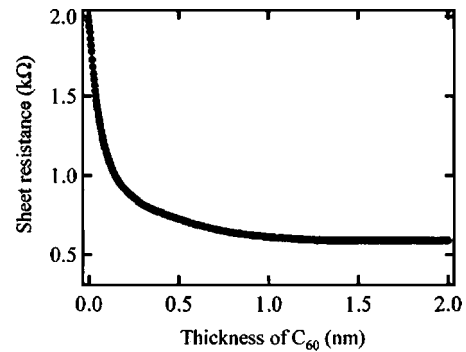


FIG. 2. Change in sheet resistance with  $C_{60}$  deposition on Ag film, with a final average thickness of 13 nm.

ever, this mechanism has little influence on the conductance change of films in the conductance range considered hereafter.<sup>4</sup> Thus, this effect is neglected in the following sections.

In stage (ii), formation of a conducting  $C_{60}$  monolayer is dominant. The charge-transfer effect makes adjacent  $C_{60}$  molecules conducting. This effect is dominant for very thin but continuous films, and it increases the sheet conductance (decreases the sheet resistance).

In stage (iii), enhancement of surface scattering gradually becomes dominant. The charge transfer gives rise to charge separation, and this separation contributes to an increase in the scattering potential of electrons at the interface between  $C_{60}$  and the metal layer. This effect is dominant for films whose resistivities are close to that of the bulk metal, and it decreases the sheet conductance (increases the sheet resistance).

In stage (iv), the metal underlayer becomes sufficiently thick that the influence of the surface effect caused by  $C_{60}$  adsorption is almost negligible. The thickness of the metal underlayer is larger than the mean free path of conduction electrons in this stage. Therefore, the surface scattering of the electrons no longer contributes significantly to the sheet resistance.

These features are fundamentally the same for other  $C_{60}$ /noble-metal systems. In Secs. III B and III C, *in situ* resistance measurements of stage (ii) in order to determine the resistance of a conducting  $C_{60}$  monolayer formed on a Ag film, and stage (iii) in order to estimate the relative amount of charge transferred across  $C_{60}$ /noble-metal (Au, Cu, and Ag) interfaces, respectively, are presented.

#### B. Resistances of conducting $C_{60}$ monolayers

If a noble-metal underlayer is sufficiently thick that an increase in resistance occurs by the deposition of  $C_{60}$  [stages (iii) and (iv) in Fig. 1], the decrease in resistance caused by the formation of a conducting  $C_{60}$  monolayer is canceled out and is hard to observe. Therefore, in order to measure the resistance of the conducting  $C_{60}$  monolayer, it is necessary to perform *in situ* resistance measurements when a decrease in resistance occurs [stage (ii) in Fig. 1].

Figure 2 illustrates the decrease in sheet resistance obtained by depositing  $C_{60}$  on a 13-nm-thick Ag film. The vertical axis indicates the sheet resistance of the  $C_{60}$ /Ag bilayer

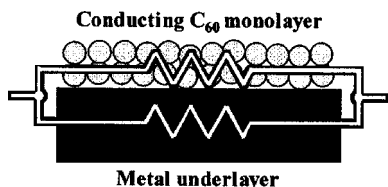


FIG. 3. Schematic diagram of resistances of a conducting  $C_{60}$  monolayer and a metal underlayer which makes a parallel connection.

film. A drastic change (71% decrease) in the sheet resistance is observed. The change in resistance is complete after the deposition of 1 nm, nearly the thickness of one monolayer of  $C_{60}$ , which represents the formation of a conducting  $C_{60}$  monolayer. This result is in excellent agreement with other works.<sup>4,10</sup>

Resistances of conducting  $C_{60}$  monolayers can be calculated by assuming that resistances of a  $C_{60}$  monolayer and a Ag underlayer make a parallel connection, as illustrated in Fig. 3. If the initial sheet resistance of a thin Ag film,  $R_i$ , is lowered to the final sheet resistance of the  $C_{60}/Ag$  bilayer,  $R_f$ , by deposition of  $C_{60}$ , the resistance of the conducting  $C_{60}$  monolayer,  $R_{ML}$ , is expressed as

$$R_{ML} = \frac{R_i R_f}{R_i - R_f}. \quad (1)$$

This parallel resistance formula gives the resistance of the  $C_{60}$  monolayer in Fig. 2 as 0.8 k $\Omega$ .

Figure 4 shows the resistances of conducting  $C_{60}$  monolayers formed on thin Ag films with various conductances. A values on the horizontal axis show the conductances of the Ag underlayers. The resistance of the conducting  $C_{60}$  monolayer decreases as the conductance of the metal underlayer increases, i.e., as the underlayer grows. The growth of noble-metal underlayers has three stages. In the first stage, the formation of metal islands is seen. Then, these islands begin to connect to each other and form a mesh structure. Finally, metal atoms cover the whole surface of the substrate and the metal film becomes completely continuous. As such, the growth of the metal underlayer implies the enlargement of the  $C_{60}$ -metal interfacial area. Thus, the more the underlayer grows, the more  $C_{60}$  molecules receive electrons from the

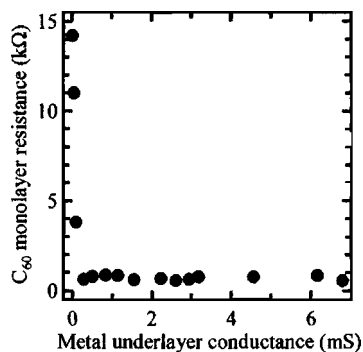


FIG. 4. Change in the resistance of a conducting  $C_{60}$  monolayer as a function of the conductance of a thin Ag underlayer. The resistances are calculated from experimental data, with the assumption that the resistances of a  $C_{60}$  monolayer and a metal underlayer make a parallel connection, as illustrated in Fig. 3.

metal film. The values of the observed plateau of the resistance curve in Fig. 4 can be attributed to the resistance of a conducting  $C_{60}$  monolayer formed on completely continuous metal films. By averaging the values in the plateau (above 0.3 mS),  $0.7 \pm 0.1$  k $\Omega$  is obtained for the resistance of the conducting  $C_{60}$  monolayer formed on the Ag underlayer.

In the previous article,<sup>4</sup> the resistances of conducting  $C_{60}$  monolayers formed on Au and Cu films were found to be  $0.9 \pm 0.2$  and  $2.4 \pm 0.4$  k $\Omega$ , respectively. Meanwhile, generally accepted values of work functions of polycrystalline Au, Cu, and Ag are 5.1, 4.65, and 4.26 eV, respectively.<sup>12</sup> As a simple consideration,  $C_{60}$  molecules on metal films with lower work functions receive more electrons from metal atoms, and the resistance of the  $C_{60}$  monolayer would be lower. Resistances obtained for conducting  $C_{60}$  monolayers, however, do not show a simple dependence upon the work functions of underlayer metals. In order to explain this result, the number of electrons donated to the LUMO with respect to the work function of the underlying metal is investigated in Sec. III C. In addition, the surface morphology of the metal underlayer, another factor in determining the resistance of a conducting  $C_{60}$  monolayer, is examined by means of AFM measurements in Sec. III D.

### C. Charge transfer across $C_{60}/noble$ -metal interfaces

In this subsection, the surface scattering cross section of conduction electrons is determined by the change in resistivity induced by  $C_{60}$  adsorption onto a metal surface. The magnitude of the cross section represents the relative amount of transferred charge across  $C_{60}/noble$ -metal interfaces because conduction electrons in the metal underlayer feel the charge transfer as an increase in the surface scattering potential.

If the film thickness is comparable to or smaller than the mean free path of conduction electrons, surface scattering effects exert a large influence on its resistivity. For continuous thin films, the resistivity can be expressed as

$$\rho = \rho_0 \left( 1 + \frac{\alpha l_0}{d} \right), \quad (2)$$

where  $\rho_0$  is the bulk resistivity, the parameter  $\alpha$  a constant which represents the degree of electron scattering at film surfaces and grain boundaries,  $l_0$  the mean free path of electrons in the bulk material, and  $d$  the film thickness. The  $d^{-1}$  dependence is known as the classical size effect.<sup>13</sup> When foreign molecules adsorb at the film surface, they act as new scattering centers for the conduction electrons. Thus, the scattering parameter  $\alpha$  increases with increasing coverage, and it follows from Eq. (2) that

$$\Delta\rho = \frac{\rho_0 l_0}{d} \Delta\alpha. \quad (3)$$

In the generally accepted theory of resistivity of thin metal films, Fuchs–Sondheimer (FS) model,<sup>14</sup> the scattering parameter  $\alpha$  is related to the parameter  $p$ , the fraction of electrons reflected specularly at the film surfaces (film–vacuum and film–substrate boundaries), as

TABLE I. The values of  $d\Delta\rho$  for noble-metal films fabricated in this study. The maximum possible values  $d\Delta\rho_{\max}$  are calculated by Eq. (6).

	$d\Delta\rho_{\max}(\mu\Omega \text{ cm } \text{\AA})$	$d\Delta\rho(\mu\Omega \text{ cm } \text{\AA})$
Au	160	$\sim 30$
Cu	120	$\sim 40$
Ag	160	$\sim 70$

$$\alpha = \frac{3}{8}(1-p). \quad (4)$$

Since  $p$  is allowed to vary only between zero and one, the resistivity increase  $\Delta\rho$  obviously cannot exceed a fixed limiting value.<sup>15</sup> During the adsorption, the electron scattering at the film-substrate boundary remains unchanged, so that the limiting value is characterized by

$$\Delta\rho_{\max} = -\frac{1}{2}, \quad (5)$$

and the maximum possible increase in resistivity becomes

$$\Delta\rho_{\max} = \frac{3}{16} \frac{\rho_0 l_0}{d}. \quad (6)$$

A scattering hypothesis proposed by Wissmann<sup>16</sup> expresses the increase in scattering parameter,  $\Delta\alpha$ , as the product of the surface density of adsorbate scattering centers  $n_a$  and the related mean scattering cross section  $\Sigma$ . Therefore, the increase in resistivity becomes

$$\Delta\rho = \frac{\rho_0 l_0}{d} n_a \Sigma. \quad (7)$$

It is obvious from this equation that the scattering hypothesis has a significant deviation from FS model because  $\Delta\rho$  has no limiting value. However, this hypothesis can be applied to the resistivity change resulting from adsorption of molecules onto metal films with very rough surfaces, e.g., cold-deposited metal films, whose value of  $\Delta\rho$  can exceed the maximum change predicted by FS model.<sup>15,17</sup>

Table I shows  $d\Delta\rho$  values of noble-metal films fabricated in this study. The values of  $d\Delta\rho$  are obviously below the theoretical maximum values calculated by Eq. (6) [using calculated free-electron parameters,<sup>18</sup> the values of  $\rho_0 l_0$  are 8.39, 6.60, and 8.43 ( $10^{-12} \text{ cm}^2$ ) for Au, Cu, and Ag, respectively]. Hebard *et al.*<sup>10</sup> estimated the surface scattering cross section of  $\text{C}_{60}$  adsorbates on a Cu film by means of the scattering hypothesis. However, metal films in this study can be described within the framework of FS model, and a method other than the scattering hypothesis is needed to estimate the scattering cross section for  $\text{C}_{60}$ /noble-metal systems investigated in this study. A commonly measured parameter in resistivity measurements is the initial slope of the resistivity change versus the surface density of adsorbates, which depends on the adsorbate-substrate system.<sup>19</sup> This has been interpreted in terms of an effective cross section for diffusive scattering of conduction electrons by the adsorbate,<sup>20</sup> defined by

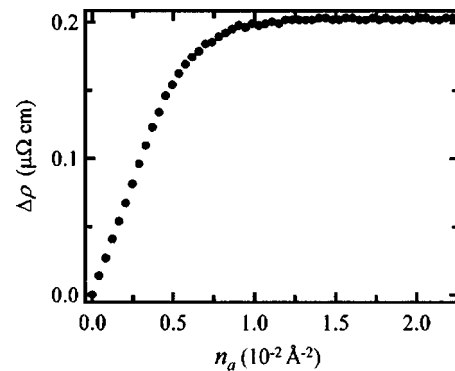


FIG. 5. The apparent change in film resistivity  $\Delta\rho$  as a function of  $\text{C}_{60}$  coverage for a 15-nm-thick Au film.

$$\Sigma = \frac{16 ne^2 d}{3 m v_F} \left. \frac{\partial \rho}{\partial n_a} \right|_{n_a \rightarrow 0}, \quad (8)$$

where  $n$  is the conduction electron density in the metal,  $e$  the unit charge,  $m$  the effective electron mass, and  $v_F$  the Fermi velocity.

Figure 5 shows the increase in resistivity obtained by depositing  $\text{C}_{60}$  on a 15-nm-thick Au film. The change in resistivity is almost complete after the deposition of one monolayer which corresponds to a surface density of  $1.11 \times 10^{-2} \text{ \AA}^{-2}$  if the  $\text{C}_{60}$  overlayer is close packed with 10.2- $\text{\AA}$  nearest-neighbor separations as in the bulk crystal of  $\text{C}_{60}$ .

As described in Eq. (8), the initial slope of the change in resistivity is needed to determine the scattering cross section  $\Sigma$ . However, the recorded data (Fig. 5) are not suitable for this purpose. The apparent change in resistivity includes contributions from two different changes: namely, resistivity increase by the surface scattering of conduction electrons from adsorbates, and resistivity decrease by the formation of a conducting  $\text{C}_{60}$  monolayer. Therefore, to determine the value of  $\Sigma$ , it is necessary to subtract the resistivity-decrease effect. The decrease effect alone can be acquired from a measurement of the  $\text{C}_{60}$  adsorption onto a thinner metal film (cf. Sec. III B or Ref. 4) because the scattering length of conduction electrons in the thinner film is so short that the surface scattering phenomenon gives rise to almost no additional resistivity (this is ensured by the observed plateau in Fig. 4). After this subtraction process, resistivity data suitable to evaluate  $\Sigma$  can be obtained, as in Fig. 6. The straight line indicates the initial slope of the change in resistivity.

As mentioned above, the cross section  $\Sigma$  is system specific. Therefore, according to Eq. (8),

$$\left. \frac{\partial \rho}{\partial n_a} \right|_{n_a \rightarrow 0} \propto 1/d, \quad (9)$$

for the same adsorbate-substrate system if it is assumed that  $\Sigma$  is independent of  $d$ , as expected, if the metal film is thick enough. This relation is well represented in Fig. 7. The straight line has the slope  $-1$  as expected for a log-log plot; this line was determined by the least-squares method. From this regression line, we obtained

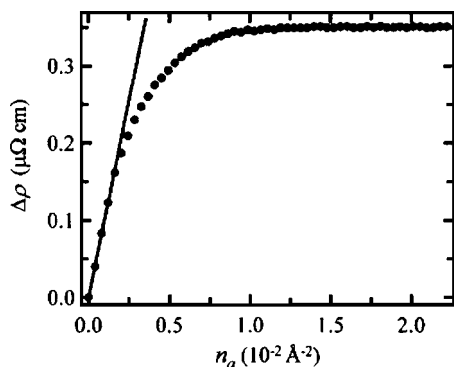


FIG. 6. The change in film resistivity due only to the increase in the surface scattering of conduction electrons. The resistivity-decrease effect by the formation of a conducting  $C_{60}$  monolayer is subtracted from the data shown in Fig. 5. The straight line indicates the initial slope of the change in resistivity.

$$d \left. \frac{\partial \rho}{\partial n_a} \right|_{n_a \rightarrow 0} \approx 1.5 \times 10^4 (\mu\Omega \text{ cm } \text{\AA}^3), \quad (10)$$

and using the values of the free-electron model<sup>18</sup> and assuming a value of  $m$  identical to the free-electron mass (these assumptions are reasonable for noble metals used in this study) give  $\Sigma \approx 100(\text{\AA}^2)$ . By the same procedure, the values of the scattering cross section  $\Sigma$  are found to be  $150 \text{\AA}^2$  for both  $C_{60}/\text{Cu}$  and  $C_{60}/\text{Ag}$  systems. These values are one order larger than other chemisorption systems.<sup>20</sup> However, considering that the charge redistribution at interfacial area between  $C_{60}$  and noble-metal (111) surfaces ranges over  $\sim 50 \text{\AA}^2$ ,<sup>21,22</sup> these values are not unreasonable for the scattering cross sections of conduction electrons.

Obtained cross sections which relatively represent the amounts of transferred charge do not show a simple dependence on the work function of the underlayer. The charge transfer from Au underlayer, with the highest work function, is the smallest as expected intuitively. There is, however, no difference in the amounts of transferred charge between Cu and Ag underlayers. This result is consistent with the direct observation by ultraviolet photoelectron spectroscopy (UPS), in which the amounts of charge transfer across the  $C_{60}$ /polycrystalline noble-metal interfaces were determined as 1.8 electrons for Cu, 1.7 for Ag, and 1.0 for Au

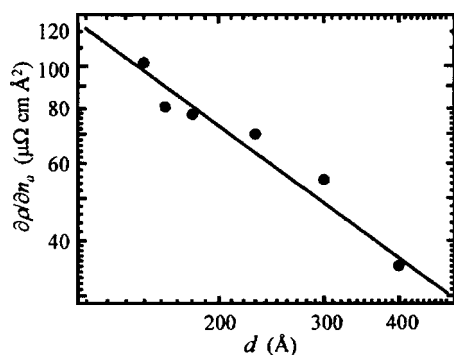


FIG. 7. The initial slope of the change in resistivity,  $\partial\rho/\partial n_a$  ( $n_a \rightarrow 0$ ), vs the film thickness of Au films,  $d$ , plot. The straight line is a regression fit with a slope of  $-1$ .

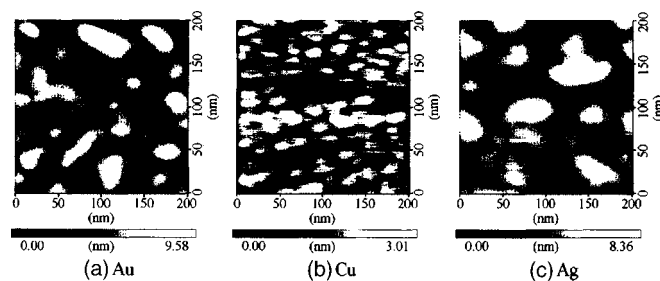


FIG. 8. AFM scans of 50-nm-thick (a) Au, (b) Cu, and (c) Ag films deposited onto quartz glass substrates.

substrates.<sup>23</sup> These results can be considered as a consequence of differences in the strength of the hybridization of the LUMO with the substrate  $sp$  band.<sup>2,23</sup>

#### D. Effect of surface morphology of metal underlayer

Besides the amount transferred charge, the surface morphology of the metal layer also has an effect on the resistance of conducting  $C_{60}$  monolayers. Figure 8 shows the surface morphologies of 50-nm-thick noble-metal films. The difference in grain size among these three metal films can be seen from these scans. The size obviously decreases for the series Ag, Au, and Cu. This fact also appears in percolation threshold for conduction (Fig. 9). These differences in the grain size and the threshold result from the difference in wetting between these metals and the quartz glass substrate. Parameters of film morphologies determined by AFM measurements are summarized in Table II. The grain concentration was roughly estimated from AFM scans shown in Fig. 8. Although the Cu film has the smoothest surface, conducting  $C_{60}$  monolayers formed on Cu films have the highest resistance. This fact implies that the grain concentration plays an important role.

At the initial stage of  $C_{60}$  growth on (111) surfaces of Au, Cu, and Ag, the  $C_{60}$  molecules adsorb exclusively at step edges.<sup>24</sup> This can hold for the present study. Since the (111) surface of fcc crystals is the most closely packed and energetically stable,<sup>20</sup> it is expected (and found experimentally) that the surface of a noble-metal film deposited at room temperature is predominantly (111). A metal grain in such a metal film has an almost square shape and the film thickness

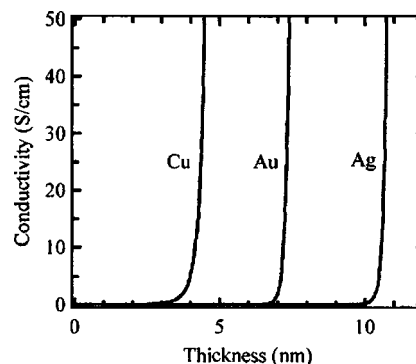


FIG. 9. Thickness dependence of conductivity of noble-metal films on quartz glass substrates measured by the two-probe method. The difference in percolation threshold for conduction results from the difference in wetting between these metals and the quartz substrate.

TABLE II. Film morphologies determined by AFM measurements on the noble-metal films shown in Fig. 8.

	rms roughness (nm)	Peak-valley (nm)	Grain concentration ( $10^{-4} \text{ nm}^{-2}$ )
Au	1.5	10.6	$\sim 9$
Cu	0.8	6.7	$\sim 22$
Ag	1.5	9.1	$\sim 7$

(height) fluctuates mainly near grain boundary.<sup>16,17</sup> Therefore, a film with higher grain concentration (with smaller grain size) is expected to have more step edges. If the charge transfer to  $C_{60}$  at step edges is smaller than that on other adsorption sites, the curve of resistivity change due to  $C_{60}$  adsorption should have an s-shaped profile like CO adsorption on a Cu(111) surface.<sup>19</sup> The s shape was observed only on the  $C_{60}/\text{Cu}$  system, as shown in Fig. 10. Although this should occur on all systems investigated in this article, the high deposition rate (about four monolayer/min) and lower grain concentration might have prevented the observation of the s shape on  $C_{60}/\text{Au}$  and  $C_{60}/\text{Ag}$  systems.

The scattering cross section of the  $C_{60}/\text{Cu}$  system, obtained in Sec. III C, was determined by the solid straight line in Fig. 10. Properly speaking, this procedure has a deviation from Eq. (8). However, the linearity of the range fitted by the line ensures that it is reasonable to determine the cross section from the “second” slope of the change in resistivity.<sup>16</sup> The broken line determines the scattering cross section for  $C_{60}$  adsorbed mainly at step edges. Employing the same procedure as in Sec. III C, the cross section of  $\sim 40 \text{ \AA}^2$  is obtained. This value is even smaller than that of the  $C_{60}/\text{Au}$  system. Therefore, higher concentration of metal grains in a Cu film indicates that less number of  $C_{60}$  molecules are “fully” electron donated from metal underlayers. This is why the resistance of conducting  $C_{60}$  monolayers formed on Cu is smaller than the resistances of  $C_{60}$  monolayers formed on Au and Ag.

In order to explain the resistance measurement results for Au and Cu, a method to estimate the number of transferred electrons for alkali fullerenes, which uses Raman shifts of the charge sensitive  $A_g(2)$  pentagonal breathing mode of

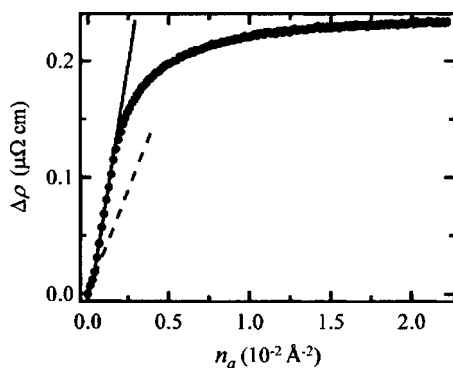


FIG. 10. The change in film resistivity  $\Delta\rho$  as a function of  $C_{60}$  coverage for a 20-nm-thick Cu film. The resistivity-decrease effect by the formation of a conducting  $C_{60}$  monolayer is subtracted and the change due only to the increase in the surface scattering of conduction electrons is shown. The straight lines indicate the slopes of the change in resistivity.

$C_{60}$  molecules, was adopted for the  $C_{60}$ -noble-metal systems in the previous article.<sup>4</sup> In the present work, however, this method has not been employed as it is not suitable for  $C_{60}$ -noble-metal systems. This is for the following reasons. The results of surface enhanced Raman-scattering (SERS) experiments<sup>25</sup> showed that the shifts of the  $A_g(2)$  mode of  $C_{60}$  molecules on the Au, Cu, and Ag substrates were  $-15.4$ ,  $-23.2$ , and  $-28.3 \text{ cm}^{-1}$ , respectively. If a calibration of  $-6 \text{ cm}^{-1}$  shifts per electron transferred to each molecule, which is used for alkali fullerenes,<sup>26</sup> is adopted for the present case, then these shifts correspond to the transfer of 2.6, 3.9, and 4.7 electrons. Employing these data, it was possible to explain the fact that a  $C_{60}$  monolayer formed on a Au film had a lower resistance than that formed on a Cu film.<sup>4</sup> However, effects other than charge transfer, such as covalent interactions, contribute to the SERS shifts, and such a local environment of the  $C_{60}$  molecule affects the charge state of the molecule.  $C_{60}$  molecules in alkali fullerenes are surrounded by metal atoms whereas those in  $C_{60}$ -noble-metal systems are not. Therefore, the calibration used for alkali fullerenes cannot be adopted for  $C_{60}$ -noble-metal systems.

In addition, it was suggested that the large amount of charge transfer in alkali fullerenes is due to the stabilization of charge state by the Madelung electrostatic energy of the crystal structure.<sup>27</sup> Actually, Hoogenboom *et al.*<sup>23</sup> performed valence-band photoemission spectroscopy on  $C_{60}/\text{polycrystalline noble-metal interfaces}$  and observed the transfer of 1.8 electrons from Cu, 1.7 from Ag, and 1.0 from Au substrates onto  $C_{60}$ . Because the  $C_{60}/\text{noble-metal bilayer}$  does not form a three-dimensional solid solution and the stabilization by the Madelung energy does not occur, these values are smaller than those obtained above by employing the calibration for alkali fullerenes.

#### IV. CONCLUSION

We performed *in situ* resistance measurements for the deposition of  $C_{60}$  molecules on a polycrystalline thin Ag film and obtained a resistance of  $0.7 \pm 0.1 \text{ k}\Omega$  for the conducting  $C_{60}$  monolayer formed on the Ag underlayer. By another series of *in situ* resistance measurements, the surface scattering cross sections of  $C_{60}$  adsorbates on polycrystalline Au, Cu, and Ag films, whose magnitude represents the relative amount of transferred charge, were evaluated as  $100 \text{ \AA}^2$  for  $C_{60}/\text{Au}$ , and  $150 \text{ \AA}^2$  for  $C_{60}/\text{Cu}$  and  $C_{60}/\text{Ag}$  systems. This behavior indicates that the number of donated electrons does not show the simple dependence upon the work functions of the metals. The result is, however, consistent with the directly observed charge transfer by means of ultraviolet photoelectron spectroscopy.<sup>23</sup> This unintuitive behavior may result from the difference in the strength of the hybridization of the LUMO with the substrate *sp* band.<sup>2,23</sup> However, comparison with previous results for monolayers formed on Au and Cu (Ref. 4) indicated that the resistances of conducting  $C_{60}$  monolayers did not show a simple dependence upon the charge transfer. Then, AFM measurements on the underlayer metals were carried out, and these showed that the difference in grain size of the underlayers can explain why the resistance of conducting  $C_{60}$  monolayers formed on Cu is smaller

than that of those on Au, despite the larger charge transfer across the C<sub>60</sub>/Cu interface. As such, there are two main factors that determine the resistance of conducting C<sub>60</sub> monolayers formed on polycrystalline noble-metal films: namely, the charge transfer and the grain size of underlayer metals. Further research is required to obtain an understanding of the relative contributions of these two factors. For instance, measurements of the resistances of C<sub>60</sub> monolayers formed on noble-metal films with different grain sizes should be carried out. Metal films with different grain size can be obtained by depositing metal atoms at different deposition rates or different deposition temperatures.

## ACKNOWLEDGMENT

This work is supported by Grants-in-Aid for Scientific Research, Japan Society for the Promotion of Science.

- <sup>1</sup>T. R. Ohno, Y. Chen, S. E. Harvey, G. H. Kröll, J. H. Weaver, R. E. Haufler, and R. E. Smalley, *Phys. Rev. B* **44**, 13747 (1991).  
<sup>2</sup>A. J. Maxwell, P. A. Brühwiler, A. Nilsson, and N. Mårtensson, *Phys. Rev. B* **49**, 10717 (1994).  
<sup>3</sup>M. R. C. Hunt, P. Rudolf, and S. Modesti, *Phys. Rev. B* **55**, 7882 (1997).  
<sup>4</sup>R. Nouchi and I. Kanno, *J. Appl. Phys.* **94**, 3212 (2003).  
<sup>5</sup>W. Zhao, K. Luo, J. Cheng, C. Li, D. Yin, Z. Gu, X. Zhou, and Z. Jin, *J. Phys.: Condens. Matter* **4**, L513 (1992).  
<sup>6</sup>X. D. Zhang *et al.*, *Chem. Phys. Lett.* **228**, 100 (1994).  
<sup>7</sup>W. B. Zhao *et al.*, *J. Phys.: Condens. Matter* **6**, L631 (1994).

- <sup>8</sup>A. F. Hebard *et al.*, *Phys. Rev. B* **50**, 17740 (1994).  
<sup>9</sup>J. Q. Wu, B. Zhao, J. Chen, K. Wu, Z. J. Wang, J. L. Zhang, C. Y. Li, and D. L. Yin, *Phys. Rev. B* **54**, 9840 (1996).  
<sup>10</sup>A. F. Hebard, R. R. Ruel, and C. B. Eom, *Phys. Rev. B* **54**, 14052 (1996).  
<sup>11</sup>H. Wang, X. Li, B. Wang, and J. G. Hou, *J. Phys. Chem. Solids* **61**, 1185 (2000).  
<sup>12</sup>H. B. Michaelson, *J. Appl. Phys.* **48**, 4729 (1977).  
<sup>13</sup>D. Schumacher, *Surface Scattering Experiments with Conduction Electrons*, Springer Tracts in Modern Physics, Vol. 128, edited by G. Höhler (Springer, Berlin, 1993).  
<sup>14</sup>E. H. Sondheimer, *Adv. Phys.* **1**, 1 (1952).  
<sup>15</sup>P. Wissmann, *Thin Solid Films* **13**, 189 (1972).  
<sup>16</sup>P. Wissmann, in *Surface Physics*, Springer Tracts in Modern Physics, Vol. 77, edited by G. Höhler (Springer, Berlin, 1975).  
<sup>17</sup>D. Dayal and P. Wissmann, *Thin Solid Films* **44**, 185 (1997).  
<sup>18</sup>C. Kittel, *Introduction to Solid State Physics*, 7th ed. (Wiley, New York, 1996), p. 150.  
<sup>19</sup>M. Hein, P. Dumas, A. Otto, and G. P. Williams, *Surf. Sci.* **419**, 308 (1999).  
<sup>20</sup>B. N. J. Persson, *Phys. Rev. B* **44**, 3277 (1991).  
<sup>21</sup>L.-L. Wang and H.-P. Cheng, *Phys. Rev. B* **69**, 045404 (2004).  
<sup>22</sup>L.-L. Wang, and H.-P. Cheng, *Phys. Rev. B* **69**, 165417 (2004).  
<sup>23</sup>B. W. Hoogenboom, R. Hesper, L. H. Tjeng, and G. A. Sawatzky, *Phys. Rev. B* **57**, 11939 (1998).  
<sup>24</sup>T. Sakurai, X.-D. Wang, Q. K. Xue, Y. Hasegawa, T. Hashizume, and H. Shinohara, *Prog. Surf. Sci.* **51**, 263 (1996).  
<sup>25</sup>S. J. Chase, W. S. Bacsa, M. G. Mitch, L. J. Pilione, and J. S. Lannin, *Phys. Rev. B* **46**, 7873 (1992).  
<sup>26</sup>M. S. Dresselhaus, G. Dresselhaus, and P. C. Eklund, *Science of Fullerenes and Carbon Nanotubes* (Academic, San Diego, 1996), p. 379.  
<sup>27</sup>E. Burstein, S. C. Erwin, M. Y. Jiang, and R. P. Messmer, *Phys. Scr.*, T **42**, 207 (1992).